ISSN 0511-5728
The West Indian Journal of Engineering
Vol.44, No.2, January 2022, pp.58-69

Quantifying Wave Runup in Data-Sparse Locations for Planning

Deborah Villarroel-Lamb [a,Ψ], and Andrew H. Williams [b]

Department of Civil and Environmental Engineering, The University of the West Indies; St. Augustine Campus, Trinidad and Tobago, West Indies;

[a]Email: deborah.villarroel-lamb@sta.uwi.edu
[b]Email: andrew.williams1@my.uwi.edu

[Ψ] *Corresponding Author*

(Received 30 June 2021; Revised: 17 December 2021; Accepted 03 January 2022)

Abstract: *The determination of wave runup is important to coastal management, including engineering designs and hazard assessments. In data-sparse regions such as the Caribbean, where critical coastal parameters are lacking for adequate decision-making, optimal use must be made of limited datasets to access continuous wave runup data. A video camera system was established at Mayaro Beach in Trinidad and collected video data for a short duration. The waterline variations were rectified and then digitised by sampling pixel intensities along a cross-shore transect. A wave runup time series of 15-minute duration was generated to represent the selected hour of video, from which statistical wave runup estimates including the maximum runup, R_{max}, and the runup exceeded by 2% of swash events, $R_{u2\%}$, were determined. Numerous expressions exist to estimate runup elevations, with the Stockdon et al. (2006) $R_{u2\%}$ predictor being a good performer. The predictive skill of this formulation was assessed, by comparing the measured and predicted magnitudes of the $R_{u2\%}$ using a calibrated/validated model for wave parameters. For the video data analysed, it was found that the coefficient of determination (R^2) and the root mean square error (RMSE) were 0.414 and 0.673m for the Stockdon et al. (2006) predictor, but improved to 0.587 and 0.055m using a modified predictor, respectively. Disparities between predicted and observed values were attributed primarily to site-specific conditions and the lack of concurrent in-situ wave data and beach slope characteristics; these were accounted for using the modified predictor and thus enabled an improved wave runup description at the data-sparse site.*

Keywords: *Video Camera; Image Processing; Wave Runup; Remote Monitoring; Coastal Risk; Beach Data.*

1. Introduction

The coastal regions are the world's most dynamic yet vulnerable areas. Management of our coastal zones require skill, knowledge and expertise to construct and maintain coastal structures and other protective measures, as well as, reduce the risks and impacts associated with shoreline erosion and shoreline flooding (Villarroel-Lamb et al., 2014). However, with the growing concern of global warming, the risk to our coastal areas will escalate with expected rises in sea level and increased frequency and intensity of extreme storm events. Additionally, coastal populations are growing, with an associated increased implementation of coastal structures to mitigate adverse impacts. All these combined factors will augment the losses expected from coastal hazards (Sale et al., 2008; UN-Oceans, 2016). Small Island Developing States (SIDS), such as many islands in the Caribbean region, are required to implement decisive solutions on their coastlines.

Expectedly, the choice of the selected action depends on the technical, social, environmental and economic feasibility of the proposed solutions. The rigour of these assessments relies heavily upon the quality and quantity of the datasets available. Beach data is critical to the assessment of mitigation and adaptation strategies for coastal environments (Valentini et al., 2017). Access to quality datasets is critical, particularly in the face of uncertain climate changes (Mummery, 2016). For activities in the coastal zone, some main objectives of data collection are to assemble meaningful datasets that can describe existing conditions well, assess trends and patterns, predict possible future outcomes and facilitate the implementation of effective solutions. Usually, this requires access to multiple datasets that have been evaluated for accuracy, reliability and suitability of purpose. Coastal practitioners must aim to assess and implement technologies and innovations that can achieve these data collection goals.

A comprehensive coastal monitoring plan should include diverse datasets including physical, chemical, ecological and social parameters. Physical parameters will normally comprise of measurements on meteorological, oceanographic and environmental indicators. Additionally, coastal conditions at the site should be described in terms of offshore and nearshore characteristics to provide a detailed overview. However, in data-sparse locations, such as many Caribbean coastlines, decision-making is based on limited data.

There are diverse types of methods for data collection, ranging from solely in-situ measurements to remote sensing techniques only, or some combination of the two approaches (Splinter et al., 2018). The selection of the data collection method depends on, inter alia, the purpose for which the data is required, accessibility to financial and/or human resources for procurement and

https://doi.org/10.47412/GDWM2126

maintenance of deployed equipment for the required period, and the ability to process the data outputs to create valuable information. By way of example, a proposed coastal solution may require real-time data, such as the establishment of a warning system, where remote sensing techniques will be preferred rather than in-situ measurements (Tralli et al., 2005). Wave runup is usually included in a wide-ranging data collection effort for a given coastal site. It is also a feature of the swash zone which is the transitioning region between the sea and the land (Baldock, 2020). The characteristics of the swash zone hydrodynamics rely on the nearshore morphology, but it is also affected by the dominant wave conditions in the inner surf zone or the breaker zone.

Wave runup is an important parameter affecting the design of coastal structures as it can be used to predict the number of waves that will reach the crest of a structure, as well as the eventual overtopping (Schüttrumpf et al., 2009). The determination of wave runup is also important in the management of beaches as the runup determines the landward extent of wave action, or in other words, it determines the extent to which the sea would influence the land. Hence, it is frequently used in the design of beach nourishment projects, coastal flooding and hazard risk mapping and monitoring. It is also used to predict beach and dune erosion (Stockdon et al., 2006). Stockdon et al. (2006), defined wave runup as the height of discrete water-level maxima. Alternatively, it is the vertical elevation of shoreline oscillation on a beach or structure above the still water elevation which is the elevation in the absence of waves (refer to Figure 1).

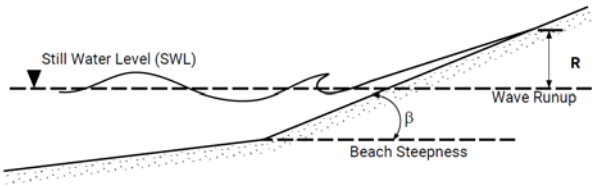

Figure 1. Definition of Wave Runup

During a runup event, also known as a swash event, the water moves in a landward direction along the beach face, known as the swash or uprush phase, and reaches a maximum position on the beach face. The water then recedes, and moves in a seaward direction which is known as the backwash or downrush phase. Investigations on measuring and predicting the magnitude of swash events began as early as 1951. Throughout this time, numerous methods have been used to measure wave runup (Bailey and Shand, 1994) and numerous predictors have been developed (Gomes da Silva et al., 2020). The various empirical formulae derived to predict this wave runup parameter have been based on both field data, as well as, laboratory experiments (Gomes da Silva et al., 2020).

Of these models, the model presented by Stockdon et al. (2006) has been described as the most accurate and widely accepted formulation to determine wave runup (Gomes da Silva et al., 2020). Recent studies have also shown that video camera recordings can be used to accurately map wave runup data and have been successfully implemented in various beach studies (Gomes da Silva et al., 2020). The position of the water level is digitised, and the time series can then be converted to vertical runup heights.

This paper investigates the use of video camera data to determine wave runup magnitudes at a coastal site. Different statistical wave runup estimates would be investigated: the minimum runup, R_{min}, the mean runup, R_{mean}, the root mean square runup, R_{rms}, the maximum runup, R_{max} and the runup exceeded by two percent (2%) of incoming waves, $R_{u2\%}$. In addition, the $R_{u2\%}$ observations would be compared to the well-recognised Stockdon et al. (2006) formulation which predicts the value of $R_{u2\%}$ based on wave and beach characteristics; limitations of the comparative analysis were documented. Finally, a modified predictor was developed and subsequently used to determine variations in wave runup over a selected calendar year which could be used for coastal planning and management.

2. Wave Runup

This section discusses the fundamental concepts of wave runup, factors that affect its magnitude and the contributing components. Additionally, various methods for wave runup data collection and assessment are detailed. Brief mention is made of the various parameterisations of wave runup, but a thorough review can be found in Gomes da Silva et al. (2020).

2.1 Overview of Wave runup

Wave runup is a result of two temporally and spatially dependent components: the time-averaged wave setup and the time-varying swash excursion. The magnitudes of these are connected to the processes that occur in the surf zone (Stockdon et al., 2006). Wave setup is defined as the super-elevation of the mean water level driven by the cross-shore gradient in radiation stresses from the breaking waves. The wave-related excess momentum flux is transferred to the water during the breaking process. Swash is the fluctuation in water levels about the mean setup level and delineates a time-varying location of the boundary between the sea and the land (Guza and Thornton, 1982).

One of the earliest works on the wave runup parameter was done by Miche (1951) where the experiments were based mainly on monochromatic waves. Miche (1951) hypothesised that the runup of monochromatic waves was related to the reflection of the coast or structure. This provided the basis of the very first empirical relationship used to describe runup which showed a positive correlation between the wave runup and the wave height. As a wave propagates towards the land, most of the wave energy is dissipated as the waves break across the surf zone. Wave energy not dissipated during the breaking process causes an increase in elevation of the mean water level across the surf zone

with a maximum at the shoreline. Some of this retained wave energy is converted to potential energy in the form of runup on the foreshore of the beach (Hunt, 1959; Gomes da Silva et al., 2020).

On natural beaches, gravity and infragravity waves can contribute to swash zone hydrodynamics including wave runup magnitudes. Gravity band waves are waves with shorter wavelengths and include wind waves and swell waves. Infragravity band waves are longer waves which can result from wave-wave interactions, or propagate from offshore areas. While both types of waves may exist in coastal areas, one type may be dominant. On beaches that can be characterised as intermediate or reflective beaches, the gravity band wave energy dominates, and waves can reach the coast in the form of bores (or shore-breaks) (Hughes et al., 2014; Baldock, 2020). These bores collapse at the beach, resulting in the runup motion often seen as a thin sheet or layer of water, with a fast-propagating wave front (Hughes et al., 2014; Baldock, 2020).

On dissipative beaches, there may be a prevalence of infragravity wave energy and this band of wave energy also influences the wave runup in the swash zone. However, a limit exists for gravity band waves as there is runup saturation at breaking, and any additional incident gravity band wave energy is dissipated across the surf zone (Ruessink et al., 1998). Therefore, on natural beaches, the contribution to wave runup at sea/swell frequencies is usually saturated, and runup in this wave energy band does not increase further with increasing wave height. Conversely, wave energy in the infragravity wave band remains unsaturated in the swash zone and consequently wave runup contributions from the infragravity frequencies are unsaturated (Huntley et al., 1977; Fiedler et al., 2019).

Furthermore, wave runup can be considered as a statistical quantity which inherently necessitates a probabilistic description and parameters such as R_{max} and $R_{u2\%}$ are used. Research done by Ahrens and Titus (1978) and Nielsen and Hanslow (1991) suggests that a Rayleigh distribution is a reasonable fit to the wave runup data. An assumed cumulative frequency distribution function for the wave runup allows for a simplified means to extract statistical quantities for design or site characterisation (Ahrens and Titus, 1978).

2.2 Methods for Collecting Wave Runup Data

Various field measurement techniques can be used to accurately determine wave runup in coastal areas. Some of these methods include point instruments such as pressure sensors or ultrasonic sensors, and Geographic Information Systems (GIS) which use measuring techniques such as photogrammetry and LIDAR (Baldock, 2020). Other common methods include traditional surveying techniques, resistance wire gauges (also known as runup wires) and video camera imagery.

Traditional surveying techniques involve the collection of data through visual observations and total station surveying techniques. The cross shore transect is established and the maximum runup within the established lines is observed. The traditional surveying technique is commonly used to establish the foreshore beach slope (Brathwaite and Villarroel-Lamb, 2020). The data collected is then geo-referenced and reduced to mean sea level data. Dual resistance wires or runup wires are usually placed across the beach face. These are analog sensors, but the output can be easily digitised. The data is then retrieved, from the runup sensors, by telemetering the data to a tape recorder or a receiver (Holman and Guza, 1984). While dual resistance wires have been used by various researchers (Guza and Thornton, 1982; Holman and Guza, 1984), there are disadvantages to using this method. Phase errors can occur at higher frequencies and the apparatus can be disturbed on site (Bailey and Shand, 1994); Guza and Thornton (1982) found that this technique was easily ruined by external factors. If video camera data is recorded using digital cameras, the runup can then be mapped by determining the swash front on the individual frames. This method can be cost efficient and can allow for runup estimates during high energy conditions such as storms (Bailey and Shand, 1994). This method is also useful to measure and quantify alongshore variations due to morphology changes. To add to this, beach phenomena can be visually observed.

To extract the runup, Schimmels et al. (2012) used video sequences collected at twenty-five (25) frames per second (fps) as described by Aagaard and Holm (1989). The individual frames may be sub-sampled at lower frequencies such as 1 to 5 fps. (Schimmels et al., 2012; Stockdon et al., 2006). Pixel intensities may be sampled along a given transect to generate the time stack images and converted to metric units using ground-truthing data. The time stack images would then be analysed. Schimmels et al. (2012) used an open-access Graphical User Interface (GUI) software developed in Matlab for processing. Though very useful, disadvantages of using the video camera method include the laborious aspect of the data processing, the difficulty in tracking swash oscillations and the need to have ground-truthing data for verification.

In addition, the resolution of the camera, along with the height and distance of the camera from the swash zone can cause errors when trying to distinguish the extent of the uprush. The cameras can also be affected by natural conditions such as rain and fog which would lower visibility, as well as, lack of daylight (Aagaard and Holm, 1989). Nonetheless, video camera data has become a proven and invaluable tool used by scientists for remote sensing of various parameters in the coastal environment, including measuring morphological change, estimating surf zone hydrodynamics parameters, measuring beach attendance and safety indicators, and the detection of marine debris (Dusek et al., 2019). While more established systems, such as Argus systems, have been available since the 1980's, low-cost alternatives (such as those using web cameras or smart phones) provide a remote and inexpensive alternative to collect critical coastal parameters at sites (Dusek et al., 2019).

There are discrepancies in the wave runup values obtained from the various methods. Ruessink et al.

(1998) explained that there were significant variations in the results obtained by similar experiments using different data collection techniques which included methods such as video images and runup wires. Schüttrumpf et al. (2009) found that the video camera data produced a higher runup than the resistance wires.

2.3 Existing Parametrisations and Factors that Affect Runup

Various predictors have been formulated in attempts to accurately predict the wave runup. These empirical formulae describe runup based on the different factors that influence its magnitude such as wave reflection, swash saturation, Iribarren number, beach slope, shape of the wave spectra, the random nature of waves, the effects of gravel and rocky beaches compared to sand beaches, the effect of fetch limited areas, wave setup and longshore variability (Gomes da Silva et al., 2020). The permeability of the bed is another factor that affects runup. Villarroel-Lamb et al. (2014) found a distinct relationship between the runup and the porosity of the beach slope. Coastal sites undergoing erosion usually exhibit a coarsening of the beach sediment as finer particles are washed away (Meadows and Campbell, 2013) and this can lead to an increased hydraulic conductivity of the beach face which is more influenced by infiltration (Bujan et al., 2019). Additionally, the nearshore bathymetry and processes, such as the presence of sands bars and cusps, affect the runup. All these factors contribute to the wave runup to different degrees.

In some total runup expressions, there is also a lack of information on the components of runup (setup and swash) that are contributing to the magnitude estimate. Unfortunately, in many of the current expressions the factors affecting the runup are not accurately quantifiable and many wave runup expressions do not include contributions from all relevant phenomena. Since it is not clear which excluded contributing factor is significantly affecting an estimate, it makes improving the runup estimate quite difficult (Gomes da Silva et al., 2020). A comprehensive assessment of various runup formulae, including the Stockdon et al. (2006) formula, was done by Gomes da Silva et al. (2020). Of all the existing models, the Stockdon et al. (2006) model was described by Gomes da Silva et al. (2020) as the most accepted method of calculating runup. This was concluded after a database of secondary field measurements was used to compare numerous predictors. The Stockdon et al. (2006) model was found to be the best overall predictive performer when compared to the other predictors in terms of estimating the total runup, swash and wave setup.

For the formulation presented by Stockdon et al. (2006), the swash and runup measurements were a compilation of data collected from ten (10) different field studies. However, the majority of the data analysed was collected at the U.S. Army Corps of Engineering Field Research Facility (FRF) in Duck, NC, USA where the beach displayed intermediate to reflective conditions. The swash motion was also influenced by an offshore sandbar and the beach had a mean foreshore slope of 0.1. These conditions tend to influence the parametrisation, resulting in a lower correlation when tested on other beaches. All the wave runup data collected for the Stockdon et al. (2006) experiments were done by means of video techniques. Simple parameters such as beach slope (β_f), wave period (T) and offshore significant wave height (H_o) were used to derive the formula. By analysing the bulk runup statistics, the following empirical formula (Eq. 1) was obtained for the $R_{u2\%}$ on natural beaches:

$$R_{u2\%} = 1.1\left(0.35\beta_f(H_oL_o)^{1/2} + \frac{\left[H_oL_o\left(0.563\beta_f^2+0.004\right)\right]^{1/2}}{2}\right) \quad (1)$$

As part of the assessment of the runup formulae, Gomes da Silva et al. (2020) used scatter plots between measured and calculated $R_{u2\%}$, and a line where the measured and predicted values were equal was shown for ease of comparison. This data presentation gave a useful indication of whether the estimated values were over-predicting or under-predicting, compared to the measured values. The Coefficient of Determination (R^2) was also used to determine the proportion of variance between the variables (and hence the correlation between the values) to illustrate how well the predictions aligned to the measurements. The Root Mean Square Error (RMSE) was also used to determine the accuracy of the runup model. Gomes da Silva et al. (2020) stated that the Stockdon et al. (2006) formula had a Coefficient of Determination (R^2) of 0.60 and a RMSE of 0.48m when comparing the measured and predicted 2% runup exceedance values.

3. Methodology

A video camera system (at approximately 10.310106°N 60.995026°W) consisting of three cameras at different angles was established at a coastal site on the east coast of Trinidad, in Mayaro (see Figure 2(a)). Some areas in Mayaro Bay have shown extensive erosion (Darsan et al., 2012), and the video camera system is located at an eroding site in the northern section of the bay. Studies conducted between 2004 and 2008 (Darsan et al., 2012), show the median sediment size at representative sites in Mayaro ranging between 0.20 and 0.23mm. However, data collected by the Department of Civil and Environmental Engineering between 2014 and 2018 have found median sediment sizes can reach maximum values of 0.52mm and 1.55mm at some locations.

The camera system logged the video data to a computer which was housed at the Travelling Officers Quarters owned by the Property and Real Estate Services Division, under the Ministry of Public Administration, Trinidad and Tobago. The beach camera system on the Mayaro coast is shown in Figure 2(b). All the cameras recorded data at 25 fps and this data was stored and retrieved from the site periodically. The limited internet connection to the on-site computer

was used primarily to assess whether the system was operational. For this study, video data from only the south-ward facing camera, Camera 10, was used. Individual images were extracted from fifteen (15) minute videos at a frame rate of 2Hz. Each 15-minute video segment was used as being representative of the hour from which it was extracted.

The Coastal Imaging Research Network (CIRN) Matlab Quantitative Coastal Imaging Toolbox (CIRN, 2020a) was used to facilitate the image extraction and image processing (Bruder and Brodie, 2020). Firstly, the camera's intrinsic parameters were determined using the available Camera Calibration Tool in Matlab. Subsequently, the CIRN Matlab Quantitative Coastal Imaging Toolbox used the camera's intrinsic parameters, and an established ground control point, to solve for the extrinsic parameters. This information was then used to geo-rectify all the extracted images. The rectifications were made in both local rotated and world coordinate systems. The rectification grids were then projected onto the imagery. To generate the time stack images, a single cross shore transect was identified and the pixels were sampled along the same line in every image. Colour thresholding was used to delimitate the bright and light points and hence distinguish between the water and sand. The pixel intensities were sampled along the transect line, and then stacked next to each other to generate the time stack images.

Figure 2. (a) Location of video camera site in Trinidad and (b) Mayaro Coast Beach Camera System

The CIRN Matlab runupTool Toolbox (CIRN, 2020b) was then used to track the leading edge of the swash, using an advanced Automated Edge Detection routine. Once the positions of the leading swash edges were digitised, the data was processed further in Matlab. Individual wave runup values were derived by first assuming that the Mean Sea Level (MSL) was the average of the water level oscillations. The wave runup is the vertical elevation above this reference MSL position. Various statistical values of the wave runup were determined and included the maximum runup (R_{max}), the minimum runup (R_{min}), the mean runup (R_{mean}), the root mean square runup (R_{rms}) and the standard deviation of the wave runup (R_{std}). The runup data was then assumed to follow a Rayleigh distribution and the 2% exceedance value ($R_{u2\%}$) was extracted. It should be noted that the video data provided the horizontal magnitudes of the wave runup and these horizontal values were converted to a vertical elevation using an averaged beach slope for data collected in Mayaro, but not specifically along the sampled transect location of the video data.

The comparison of the Stockdon et al. (2006) runup model to the measured data (derived from the video data) was completed using offshore wave parameters using DHI's MIKE21 coupled HD-SW model (DHI, 2021) (see Figure 3).

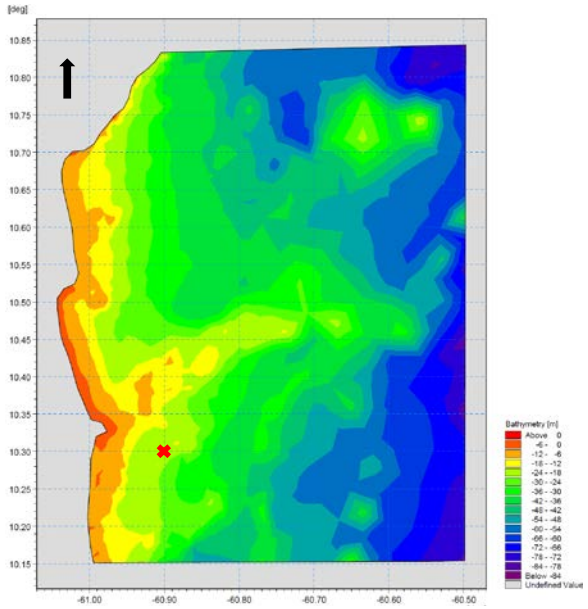

Figure 3. Mesh used for the MIKE21 Coupled SW-HD Model

The offshore eastern boundary was driven with waves obtained from the WaveWatch III (WW3) Global Wave Model and winds over the computational domain that were derived from the NOAA/NCEP Global Forecast System (GFS) Atmospheric Model. WW3 Waves and GFS Winds were obtained from the ERDAPP Data Server for the time periods modelled (NOAA, 2021). Water level variations in the MIKE21 model were assumed to be tidal and these were derived using the Tidal Toolbox in MIKE21 for all non-land

boundaries. The model was calibrated with measured wave data collected from November 2016 to March 2017 at a location in Mayaro: Mayaro Pt.1- 10.292337°N 60.998359°W. The calibrated model output was validated with wave data collected in the period January 2018 to May 2018 at two proximal locations: Mayaro Pt.2-10.292349°N 60.998313°W and Mayaro Pt.3- 10.292328°N 60.998268°W (see Figure 4).

For the wave runup estimates using the Stockdon et al. (2006) predictor, wave data was extracted at a location offshore of the video cameras (10.3°N 60.9°W), in about 20.7m water depth, and was used as representative offshore wave conditions at the Mayaro coast (see Figure 3). These modelled waves were used as a proxy to measured wave parameters as no in-situ wave gauge was deployed in the Mayaro coastal zone at the time of the video data collection. Care was taken in the extraction of these temporally-varying datasets as the MIKE21 model provided wave data at UTC, while the video data was recorded in local time (-4hrs UTC). The significant wave heights and the average wave periods were extracted from the model and used as the representative offshore wave heights (H_o) and wave periods. The wave period was then used to calculate the offshore (or deepwater) wavelength (L_o) using Eq. 2

.

$$L_o = \frac{gT^2}{2\pi} \tag{2}$$

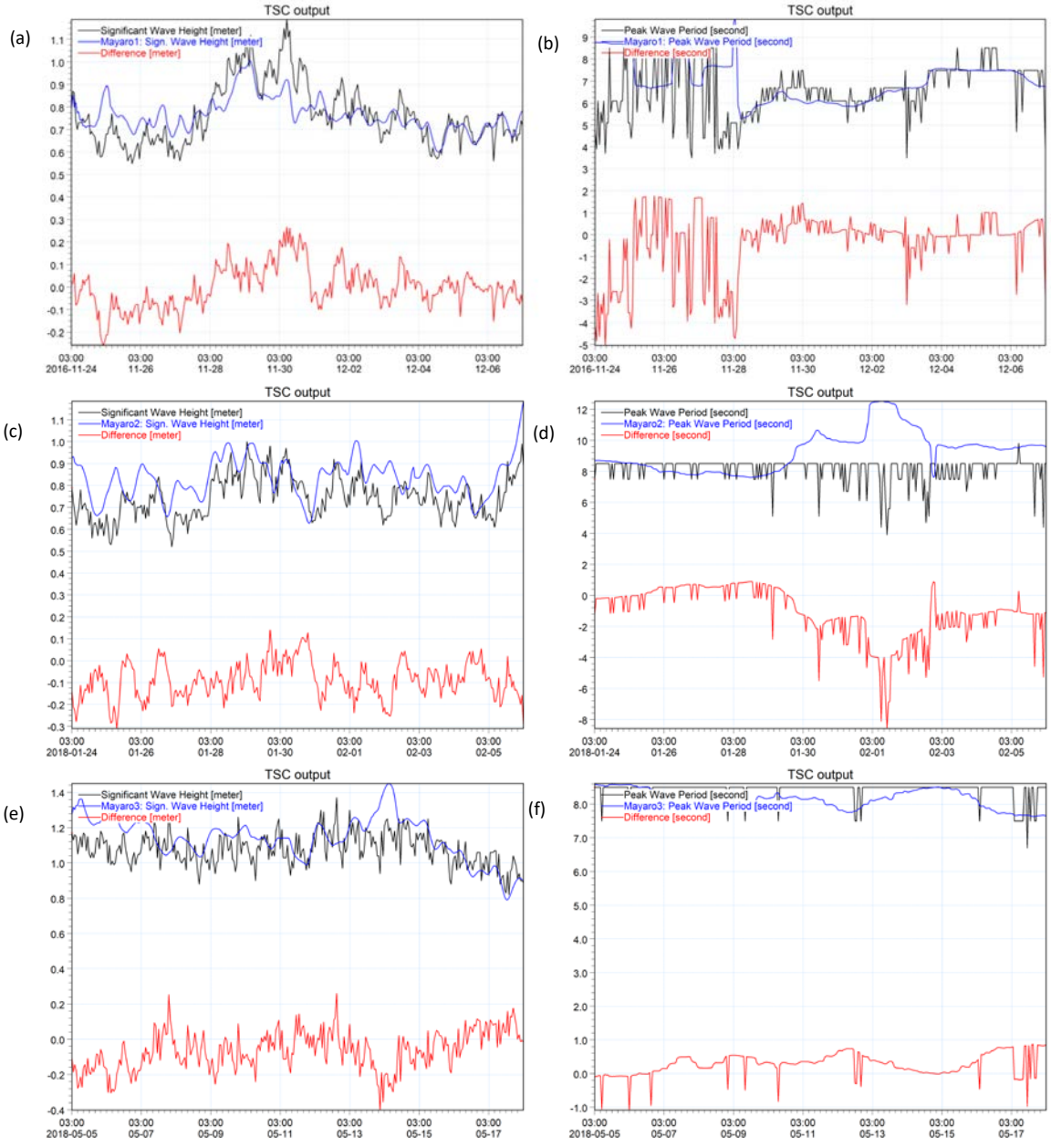

Figure 4. Summary of output from the MIKE21 wave model calibration (a), (b) at Mayaro Pt.1 and validation (c), (d), (e), (f) at Mayaro Pt.2 and Mayaro Pt.3

The skill of the Stockdon et al. (2006) model was assessed using the scatter plot of the measured and predicted values, as well as the R^2 and the RMSE values. The Coefficient of Determination (R^2) was calculated using the formula in Eq. 3.

$$R^2 = \left(\frac{n(\sum xy) - (\sum x)(\sum y)}{\sqrt{[n(\sum x^2) - (\sum x)^2][n(y^2) - (\sum y)^2]}} \right)^2 \quad (3)$$

where y represents the predicted runup values and x represents the measured runup values.

The Root Mean Square Error (RMSE) was calculated using Eq. 4.

$$RMSE = \sqrt{\frac{[\sum_{i=1}^{N}(Predicted_i - Actual_i)^2]}{n}} \quad (4)$$

Following on from the comparative assessment with the Stockdon et al. (2006) model, a modification was applied to the Stockdon et al. predictor in order to account for the limitations due to the lack of in-situ wave data and beach face data, as well as, any site-specific characteristics. The modification used a global multiplier applied to the Stockdon et al. (2006) formula and was based on the product of a dimensionless constant, C_{runup}, and a modified wave height, $H_{o\text{-}mod}$. $H_{o\text{-}mod}$ was equal to H_o divided by a constant C_{wave}. Eq. 5 below summarises the modified predictor, $R_{u2\%-mod}$, where $R_{u2\%}$ is the Stockdon et al. (2006) formula given in Eq. 1.

$$R_{u2\%-mod} = C_{runup}\left(\frac{H_o}{C_{wave}}\right) R_{u2\%} \quad (5)$$

4. Results and Discussion

The still images from each 15-minute segment were first extracted from the video data, and a sample image is shown in Figure 5. The timestack images were obtained for each 15-minute segment from selected hourly periods and were representative of that hour. Timestack images were processed using the CIRN Matlab runupTool Toolbox (CIRN, 2020b).

Figure 5. Still Image from Video Data at Mayaro

The main results from the CIRN Matlab Quantitative Coastal Imaging Toolbox (CIRN, 2020a) are shown in Figures 6, 7, 8 and 9. Figure 6 shows the grid rectifications for the rotated local and real-world coordinate systems for the still image shown in Figure 5, while Figure 7 shows the bright, dark, and average pixel intensities used to track the position of the leading swash edge. Figure 8 shows the location of the selected cross-shore transect used to determine the runup for the beach and Figure 9 shows the resulting timestack image from the selected transect for that selected 15-minute segment. Figure 10 shows the digitisation of the leading swash edge of the time stack image using the CIRN Matlab runupTool Toolbox (CIRN, 2020b).

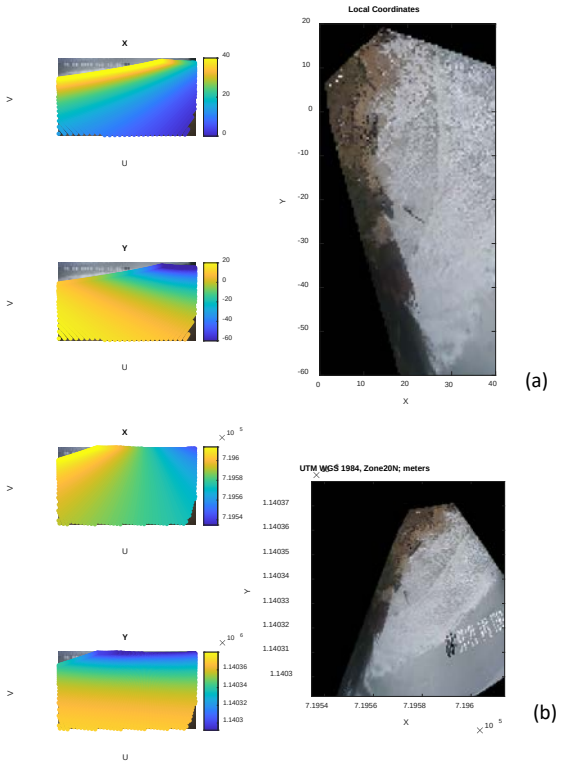

Figure 6. Grid Rectifications for Rotated Local (a) and Real World (b) Coordinate Systems

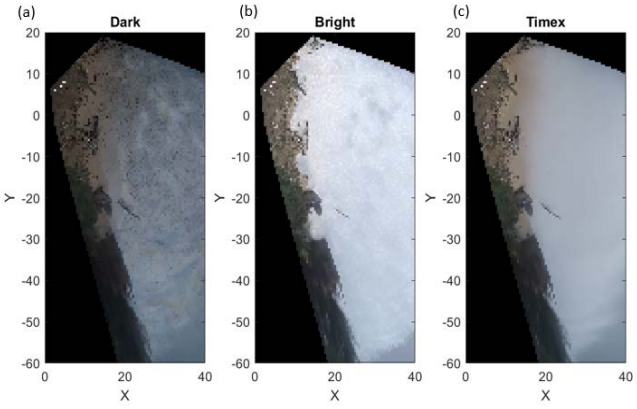

Figure 7. Statistical Image Products for Minimum Intensity (a) Maximum Intensity (b) and Average Intensity (c) of the Pixels in the Local Rotated Coordinate System

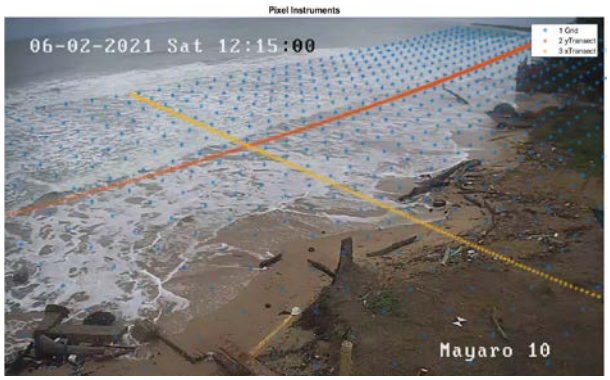

Figure 8. Establishment of Cross-Shore Transect (or x-Transect)

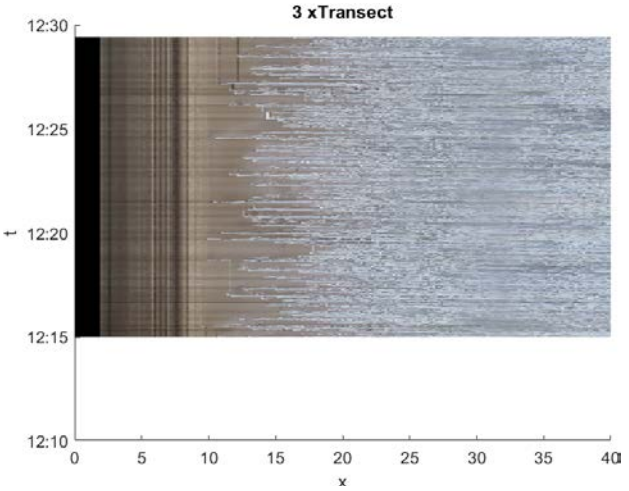

Figure 9. Resulting Time Stack Image for Cross-Shore Transect (or x-Transect)

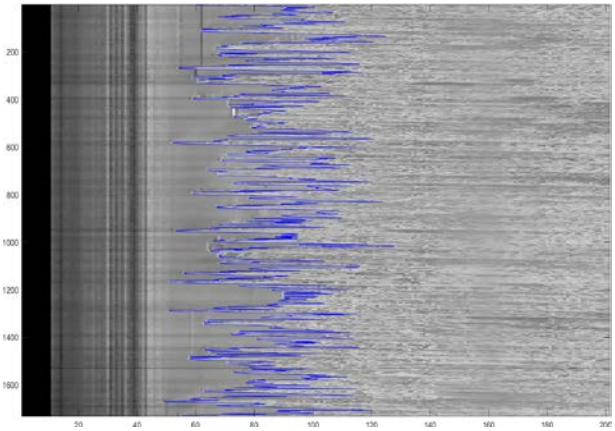

Figure 10. Detection of Swash Edge Boundary using runup tool

Further processing of the output from the CIRN Matlab runupTool Toolbox (CIRN, 2020b) yielded the various statistical estimates of the measured wave runup. Table 1 summarises some of the statistical runup values extracted from the video camera data. Figure 11 (a) shows the determination of the MSL from the raw data which was the time-averaged water level position over the sample of video data. The runup values were taken as the water's edge in excess of the MSL position. A Rayleigh Distribution was assumed and Figures 11 (b) and 11 (c) show the resulting plots of the probability density function (pdf) and the cumulative distribution function (cdf) of the runup values respectively. The R_{max} values were the highest runup values recorded, with the $R_{u2\%}$ values being the second largest, followed by the R_{mean} values, while the R_{min} values had the smallest magnitudes. This trend was anticipated as the runup elevations should decrease from R_{max} to R_{min} and this pattern served as a quality check to ensure that the outputs from the data processing were accurate. Some other data trends were observed. Namely, the minimum runup elevation appeared to remain constant for this period of data collection, and R_{rms} values were greater in magnitude than the R_{mean} values.

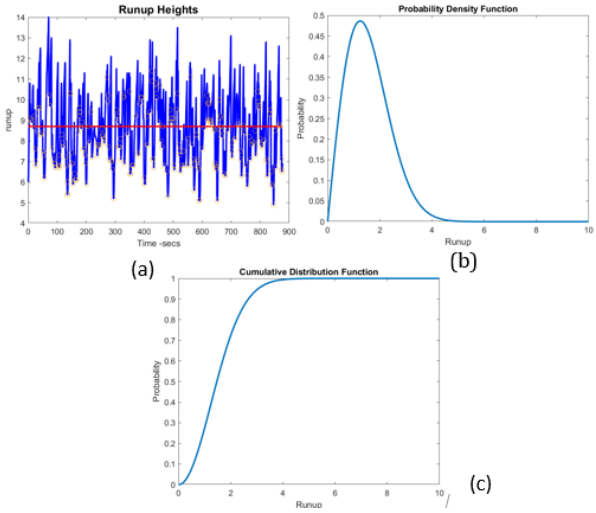

Figure 11. Runup Values with at MSL 8.7m (a), Rayleigh Probability Density Function of the Runup Values (b) and the Resulting Cumulative Distribution Function (c)

However, during data processing, there were a few errors and limitations which would have affected the accuracy of the results. Firstly, during the geo-rectification of the images, only one ground control point was used. Initially, there were two control points within the line of site of the camera but one of the control points was obscured by a fishing vessel for the video data collection period. As a result, only one ground control point was used to determine the extrinsic parameters and rectify the images. Having the two control points would have allowed the real-world coordinates to be better defined on the images increasing the accuracy of the local coordinate system used to determine the runup.

The next difficultly encountered during the processing was human and animals obstructing essential locations during the data extraction. This affected the time stack images being generated as the pixel intensities would have been skewed. These obstructions appear on the time stack images as unusually bright or dark spots or a distorted stack. This caused uncertainty when digitising the leading swash edge. In addition, the shoreline being investigated was littered with debris which would also have reduced the magnitude of the

Table 1. Measured R_{max}, $R_{u2\%}$, R_{min}, R_{mean}, R_{rms} and R_{std} extracted from Video Camera Data

Record Number	Date	Time	R_{max} (m)	$R_{u2\%}$ (m)	R_{min} (m)	R_{mean} (m)	R_{rms} (m)	R_{std} (m)
1	06-Feb	8:00	0.588	0.525	0.014	0.236	0.272	0.135
2	06-Feb	9:00	0.616	0.490	0.014	0.214	0.254	0.138
3	06-Feb	10:00	0.532	0.476	0.014	0.220	0.247	0.113
4	06-Feb	11:00	0.504	0.469	0.014	0.166	0.241	0.107
5	06-Feb	12:00	0.532	0.476	0.014	0.215	0.247	0.122
6	06-Feb	13:00	0.630	0.490	0.014	0.218	0.252	0.127
7	06-Feb	14:00	0.546	0.427	0.014	0.185	0.221	0.122
8	06-Feb	15:00	0.630	0.616	0.014	0.278	0.320	0.160
9	07-Feb	8:00	0.448	0.371	0.014	0.153	0.188	0.110
10	07-Feb	9:00	0.546	0.441	0.014	0.188	0.228	0.129
11	07-Feb	10:00	0.518	0.413	0.014	0.187	0.214	0.103
12	07-Feb	11:00	0.504	0.385	0.014	0.171	0.200	0.103
13	07-Feb	12:00	0.616	0.329	0.014	0.137	0.170	0.100
14	07-Feb	13:00	0.518	0.448	0.014	0.205	0.231	0.108
15	07-Feb	14:00	0.616	0.420	0.014	0.185	0.217	0.113

Table 2. $R_{u2\%}$ from Stockdon et al. (2006) and modified Stockdon et al. (2006) Predictors

Record Number	Date	Time	Wave Height (m)	Wave Period (secs)	Offshore Wavelength (m)	$R_{u2\%}$ (m)	$R_{u2\%\text{-mod}}$ (m)
1	06-Feb	8:00	1.645	5.920	54.73	1.143	0.472
2	06-Feb	9:00	1.625	5.982	55.87	1.147	0.468
3	06-Feb	10:00	1.607	6.000	56.21	1.145	0.462
4	06-Feb	11:00	1.600	6.111	58.31	1.163	0.467
5	06-Feb	12:00	1.598	6.048	57.12	1.150	0.461
6	06-Feb	13:00	1.604	5.980	55.83	1.139	0.459
7	06-Feb	14:00	1.619	5.924	54.79	1.134	0.461
8	06-Feb	15:00	1.633	5.943	55.15	1.143	0.469
9	07-Feb	8:00	1.572	5.661	50.04	1.068	0.421
10	07-Feb	9:00	1.593	5.661	50.03	1.075	0.430
11	07-Feb	10:00	1.595	5.717	51.03	1.086	0.435
12	07-Feb	11:00	1.589	5.763	51.85	1.093	0.436
13	07-Feb	12:00	1.579	5.825	52.98	1.101	0.436
14	07-Feb	13:00	1.565	5.957	55.40	1.121	0.440
15	07-Feb	14:00	1.550	6.043	57.01	1.132	0.440

runup. The position of the MSL was estimated as the mean of the water level oscillations and served as the reference position for the runup values.

Ideally, the MSL position should be based on the time-averaged position of the sea surface using water level measurements. The estimated position of the MSL would have been affected by any outliers resulting in runup values being smaller or larger, depending on the effect of these outliers on the MSL position. To convert the resulting horizontal runup values to a vertical elevation, the horizontal runup was multiplied by the slope of the beach. At the location of the particular transect analysed, the exact slope of the beach was unknown and assumed to be an averaged value for the Mayaro coastal area. From beach data collected at other locations in Mayaro, the slope of the beach was found to have a mean value of 0.14, a minimum value of 0.12, a maximum value of 0.15 and a standard deviation of 0.01. However, errors may be introduced to the runup if the beach slope used was not similar to the actual value along the transect. Other possible sources of error in the measured results include the use of a 15-minute segment to represent hourly measurements.

The highest sampling rate for the wave data from an ADCP is 1 reading per hour. Therefore, it was only possible to calculate a single $R_{u2\%}$ value each hour using the Stockdon et al. (2006) formula. The use of the 15-minute period was done since processing of an entire hour of video data was computationally intensive. This representation would have affected the accuracy of the results as the $R_{u2\%}$ is a statistical measure and will vary depending on the sample used. Some confidence in the representative period is provided as the standard deviations across the 15 hours sampled were on the same order of magnitude (see Table 1). It is worthy to mention that validation of the measured wave runup derived from the video camera could have been achieved with the use of another measurement technique. For example, simple surveying techniques and visual observations could have been used to determine how the runup, for a specific period, compared with the results from the video data to assure quality of the output.

The wave runup prediction using the Stockdon et al. (2006) formula is shown in Table 2 and Figures 12 and 13. The skill of the Stockdon et al. (2006) predictor in estimating the $R_{u2\%}$ values is characterised by a R^2 value of 0.414 and an RMSE value of 0.673m. It can easily be seen that the predicted values were higher than the measured values and were over-estimating the wave runup. The RMSE of 0.673m was higher than the 0.48m magnitude obtained by Gomes da Silva et al. (2020).

Also, the R^2 value of 0.414 was lower than the 0.60 value stated in Gomes da Silva et al. (2020) and indicates that the variables were not well-correlated for this study. From Figure 13, however, it can be seen that there are similar trend patterns in the data notwithstanding the errors in magnitude.

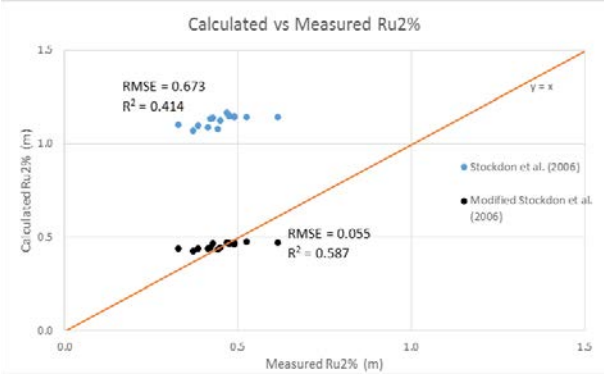

Figure 12. Predicted $R_{u2\%}$, based on Stockdon et al. (2006) and the modified Stockdon et al. (2006) vs measured $R_{u2\%}$

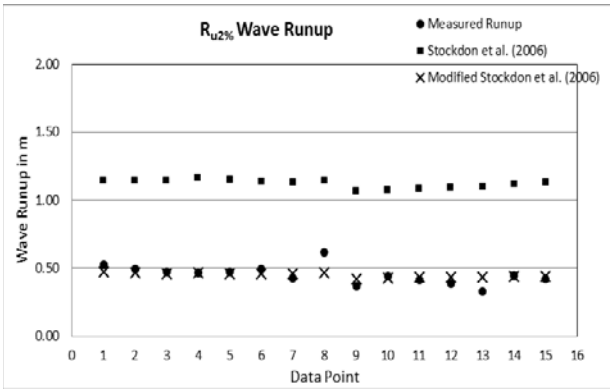

Figure 13. Predicted $R_{u2\%}$, based on Stockdon et al. (2006) and measured $R_{u2\%}$

One contributing factor to the poor correlation of the measured runup with the Stockdon et al. (2006) formula was the use of the modelled wave data. Although the modelled wave parameters did show good agreement with the measured waves during model calibration and validation, the lack of simultaneous measured wave data would have produced some unknown error in the runup predictions. In addition, the beach face characteristics were not well-described with the parameters used at the coastal site; the beach slope introduces another possible source of error. There are also attendant limitations with the Stockdon et al. (2006) formula.

Notably, the formula does not consider all the numerous factors that can affect the wave runup. The most important factors were indicated in Section 2 of this paper. However, one of the major factors that can account for the measured runup being less than the predicted runup, is that the Stockdon et al. (2006) formula does not consider the porosity of the shoreface. As the waves runup on the beach face, they also infiltrate into the bed which would decrease the magnitude of the runup. At the Mayaro site, there is a possible increase in infiltration of the swash into the beach face due to the coarsening of the sediment as a result of the ongoing erosion. Lastly, differences in wave runup magnitudes can also result from the presence of nearshore morphological features at Mayaro which can reduce wave energy at the shore.

Considering that critical coastal sites such as this one located in Mayaro bay, may continue to be lacking in-situ data for coastal assessment, a modification to the runup predictor was proposed and provided in Eq. 5. The modified predictor will allow for an improved correlation and prediction of the wave runup which can be then used for coastal management strategies. For this site, C_{runup} was determined as 0.4016, which is the averaged ratio between the observed runup and the Stockdon et al. (2006) runup for the period of the video data analysed. This modification yielded a much-reduced RMSE of 0.060m, but with a similar correlation. An improved correlation, and further reduction in RMSE was obtained by an additional modification to the Stockdon et al. (2006) runup using the multiplier, $H_{o\text{-}mod}$. For this site, C_{wave} was 1.6 which was the average value of H_o during the video data collection where $H_{o\text{-}mod}$ is effectively a dimensionless scaled wave height. The skill of the final modified Stockdon et al. (2006) predictor (Eq. 5) is exhibited by a R^2 value of 0.587 and an RMSE value of 0.055m. Table 2, and Figures 12 and 13 show the improvement in the wave runup prediction of the modified formulation.

Consequently, to illustrate the applicability of the modified predictor to coastal planning at this site, a modelled wave time series was generated for the entire year of 2020, and the modified Stockdon et al. (2006) predictor was used to generate an annual series of $R_{u2\%}$ wave runup at the location. Figures 14 and 15 show the generated annual time series and the resulting histogram of wave runup for the year 2020, respectively. Various distributions were fitted to assess optimal probabilistic descriptions to represent the wave runup at the site. This type of data output can be readily assimilated into a management strategy for the coastal site.

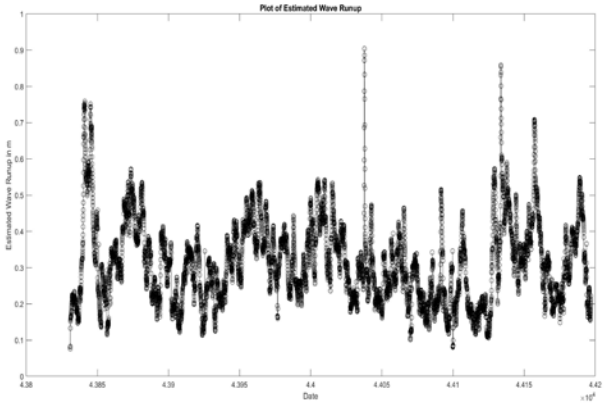

Figure 14. Predicted $R_{u2\%}$, based on the modified Stockdon et al. (2006) for 2020 presented as a time series

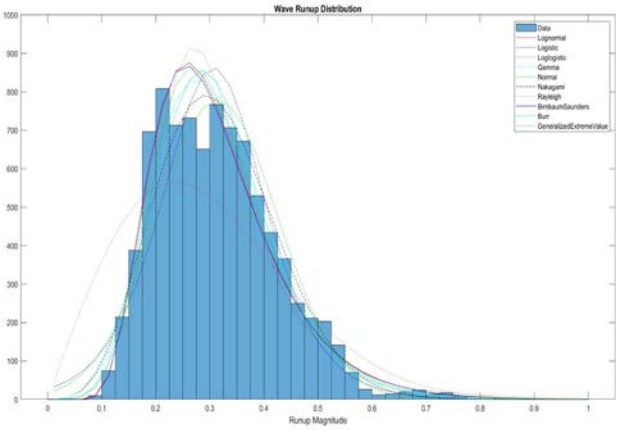

Figure 15. Predicted $R_{u2\%}$, based on the modified Stockdon et al. (2006) for 2020 presented as a histogram with fitted distributions

5. Conclusion

There are numerous factors that affect the magnitude of the wave runup causing it to vary both temporally, at a given time, and spatially at a given location along the coastline. In order to increase the confidence in runup predictions, complex formulations may aid in explaining a number of the contributing processes. However, this may not produce a practical estimator. In addition, the factors affecting wave runup are not always accurately quantifiable, and there is still uncertainty as to the phenomena that contribute to the dynamics in the swash zone. Therefore, the Stockdon et al. (2006) formula is still commonly used even with perceived limitations. The comparison between the predicted $R_{u2\%}$ values, using Stockdon et al. (2006) and the measured $R_{u2\%}$, derived from the video cameras, was not well-correlated as evidenced by the R^2 value of 0.414.

Additionally, there was a tendency by the Stockdon et al. (2006) formula to over-predict runup values as is illustrated by the RMSE was 0.673m in this study. Some uncertainty in the outputs of the comparative study still remains due to the inaccessibility to in-situ wave and beach parameters. However, this study showed that the use of a modified Stockdon et al. (2006) predictor at the coastal site to account for these uncertainties, yielded much-improved estimates for the wave runup. The modified Stockdon et al. (2006) predictor had an RMSE of 0.055m and an R^2 value of 0.587.

There are also numerous methods in which the magnitude of the runup can be measured with various levels of accuracy. Use of video cameras has become quite popular due to the remote nature of data collection, as well as the ability to obtain a continuous record of data. The method was able to yield various statistical estimates of the runup at a local site in Trinidad and produce useful output. However, runup measurements using video data is still subject to a number of limitations, spanning from the data collection through to the data processing phases. At this site, there were many practical issues such as a simultaneous proximal wave dataset and in-situ beach characteristics, security of the instrumentation, limited access to the internet and intermittent electrical or power supply. Similar practical issues will exist at other coastal sites in Trinidad and Tobago and the wider Caribbean.

Further research is required to assess the application of site-specific modified runup predictors to other local and regional coastlines, in order to augment datasets at data-sparse locations. However, this study has demonstrated that limited measured data may be used to yield a meaningful wave runup dataset that can be used for coastal planning.

Acknowledgments:

The authors acknowledge the RDI fund for sponsorship of the video camera project, and wish to recognise the Property and Real Estate Services Division, under the Ministry of Public Administration, Trinidad and Tobago for their support.

References:

Aagaard, T. and Holm, J. (1989), "Digitisation of wave run-up using video records", *Journal of Coastal Research*, Vol. 5, No. 3, pp. 547-551.

Ahrens, J. P. and Titus, M. F. (1978), "Irregular wave runup and overtopping", *Journal of the Waterway, Port, Coastal and Ocean Division*, Vol. 104, No. 4, pp. 439-442.

Bailey, D.G. and Shand, R.D. (1994), "Determining wave run-up using automated video analysis", *Proceedings of the Second New Zealand Conference on Image and Vision Computing*, pp. 2.11.1 - 2.11.8.

Baldock, T. (2020), "Swash zone dynamics", *Flanders Marine Institute (VLIZ) Coastal Wiki*, accessed 23/11/2020, available at: http://www.coastalwiki.org/wiki/Swash_zone_dynamics

Bujan, N., Cox, R. and Masselink, G. (2019), "From fine sand to boulders: Examining the relationship between beach-face slope and sediment size". *Marine Geology*, Vol. 417.

Brathwaite, S. and Villarroel-Lamb, D. (2020), "Evaluation of wave run-up predictions from parametric models on Trinidad beaches", *Proceedings of the International Conference on Emerging Trends in Engineering & Technology (IConETech-2020)*, Trinidad and Tobago.

Bruder, B.L. and Brodie, K.L. "CIRN quantitative coastal imaging toolbox", *SoftwareX*, Vol.12, pp.1-8, doi: https://doi.org/10.1016/j.softx.2020.100582.

CIRN (2020a), "CIRN-Quantitative-Coastal-Imaging-Toolbox", Coastal Imaging Research Network, available at: https://github.com/Coastal-Imaging-Research-Network/CIRN-Quantitative-Coastal-Imaging-Toolbox

CIRN (2020b), "RunupTool-Toolbox", Coastal Imaging Research Network, available at: https://github.com/Coastal-Imaging-Research-Network/runupTool-Toolbox.

Darsan J., Ramnath, S. and Alexis, C. (2012), *Coastal Conservation Project Status of Beaches and Bays in Trinidad (2004 – 2008)*, Technical Report from Institute of Marine Affairs.

Dusek, G., Hermandez, D., Willis, M., Brown, J.A., Long, J.W., Porter, D.E. and Vance, T.C. (2019), "WebCAT: Piloting the development of a web camera coastal observing network for diverse applications", *Frontiers in Marine Science*, Vol. 6, June, Aricle.353, doi:10.3389/fmars.2019.00353

Fiedler, J. W., Smit, P. B., Brodie, K. L., McNinch, J. and Guza, R. T. (2019), "The offshore boundary condition in surf zone modelling", *Coastal Engineering*, Vol. 143, pp. 12-20.

Gomes da Silva, P., Coco, G., Garnier, R. and Klein, A. H. F. (2020), "On the prediction of runup, setup and swash on beaches", *Earth-Science Reviews*, Vol. 204, pp. 1-22.

Guza, R. T. and Thornton, E. B. (1982), "Swash oscillations on a natural beach", *Journal of Geophysical Research*, Vol. 87, No. C1, pp. 483– 491.

Holman, R. A. and Guza, R. T. (1984), "Measuring run-up on a natural beach", *Coastal Engineering*, Vol. 8, No. 2, pp. 129-140.

Hughes, M.G., Aagaard, T., Baldock, T.E., and Powe, H.E. (2014), "Spectral signatures for swash on reflective, intermediate and dissipative beaches", *Marine Geology*, Vol. 355, pp. 88-97, doi: 10.1016/j.margeo.2014.05.01

Hunt, I. (1959), "Design of seawalls and breakwaters", *Journal of Waterways and Harbours Division*, Vol. 85, pp. 123-152.

Huntley, D. A., Guza, R. T. and Bowen, A. J. (1977), "A universal form for shoreline run-up spectra", *Journal of Geophysical Research*, Vol. 82, No. 18, pp. 2577-2581.

Meadows, P. S. and Campbell, J. I. (2013), *An Introduction to Marine Science*, 2nd Edition, Springer Netherlands.

Miche, A. (1951), "Le pouvoir réflechissement des ouvrages maritimes- exposés à l'action de la houle", *Annales des Ponts et Chaussees*, Vol. 121, pp. 285-319.

Mummery, J. C. (2016), "Available data, datasets and derived information to support coastal hazard assessment and adaptation planning", *CoastAdapt Information Manual 3*, National Climate Change Adaptation Research Facility, Gold Coast, Australia.

DHI (2021), "MIKE21/3", available at: https://www.mikepoweredbydhi.com/products/mike-21-3

Nielsen, P. and Hanslow, D. J. (1991), "Wave Runup Distributions on Natural Beaches", *Journal of Coastal Research*, Vol. 7, No. 4, pp. 1139-1152.

NOAA, (2021), "ERDAPP Data Server", accessed 01/06/2021, available at: https://coastwatch.pfeg.noaa.gov/erddap/index.html

Ruessink, B. G., Kleinhans, M. G. and van den Beukel, P. G. L. (1998), "Observations of swash under highly dissipative conditions." *Journal of Geophysical Research: Oceans*, Vol. 103, No. C2, pp. 3111-3118.

Sale, P.F., Butler IV, M. J., Hooten, A. J., Kritzer, J. P., Lindeman, K. C., Sadovy de Mitcheson, Y. J., Steneck, R. S. and van Lavieren, H. (2008), "Stemming Decline of the Coastal Ocean: Rethinking Environmental Management", *A Policy Brief from the United Nations University, International Network on Water, Environment and Health*, UNU-INWEH, Hamilton, Canada.

Schimmels, S., Vousdoukas, M., Wziatek, D., Becker, K., Gier, F. and Oumeraci, H. (2012), "Wave run-up observations on revetments with different porosities", *Proceedings of 33rd International Coastal Engineering Conference*, Santander, Spain, Vol. 1, No. 33.

Schüttrumpf, H., Kortenhaus, A., Bruce, T. and Franco, L. (2009), "Wave run-up and wave overtopping at Armored Rubble Slopes and Mounds", *Handbook of Coastal and Ocean Engineering*, World Scientific, Singapore.

Splinter, K. M., Harley, M. D. and Turner, I. L. (2018), "Remote sensing is changing our view of the coast: Insights from 40 years of monitoring at Narrabeen-Collaroy, Australia", *Remote Sensing*, Vol. 10, No. 11, pp. 1-25.

Stockdon, H. F., Holman, R. A., Howd, P. A. and Sallenger, A. H. (2006), "Empirical parameterisation of setup, swash, and runup", *Coastal Engineering*, Vol. 53, No. 7, pp. 573-588.

Tralli, D. M., Blom, R. G., Zlotnicki, V., Donnellan, A. and Evans, D. L. (2005), "Satellite remote sensing of earthquake, volcano, flood, landslide and coastal inundation hazards", *ISPRS Journal of Photogrammetry and Remote Sensing*, Vol. 59, No. 4, pp. 185-198.

UN-Oceans (2016), "UN Atlas of the Oceans", accessed 23/11/2020, available at: http://www.oceansatlas.org/

Valentini, N., Saponieri, A. and Damiani, L. (2017). "A new video monitoring system in support of Coastal Zone Management at Apulia Region, Italy", *Ocean and Coastal Management*, Vol. 142, No. 15, pp. 122-135.

Villarroel-Lamb, D., Hammeken, A. and Simons, R. (2014), "Quantifying the effect of bed permeability on maximum wave runup", *Proceedings of 34th International Coastal Engineering Conference*, Seoul, Korea, Vol. 1, No. 45.

Authors' Biographical Notes:

Deborah Villarroel-Lamb *is a Lecturer in the Department of Civil and Environmental Engineering at The University of the West Indies (UWI), St. Augustine, Trinidad and Tobago. She received a BSc (2000) and PhD (2007) degree in Civil Engineering from The UWI. Dr. Villarroel-Lamb is a past recipient of the Newton Internal Fellowship from the Royal Society (UK), 2009-2011 and also a Fellow of the Royal Society of Arts (FRSA). Deborah specialises in coastal engineering, which includes ocean hydrodynamics, coastal morphology and coastal engineering solutions.*

Andrew H. Williams *is a graduate of The University of the West Indies, St. Augustine and is currently a M.Sc. student in the Department of Civil and Environmental Engineering. His research interests are costal nature based solutions and the use of video camera systems for monitoring coastal processes.* ■